Harmful Algae 68 (2017) 258–270

Contents lists available at ScienceDirect

Harmful Algae

journal homepage: www.elsevier.com/locate/hal

Transcriptional response of the harmful raphidophyte *Heterosigma akashiwo* to nitrate and phosphate stress

Sheean T. Haley[a], Harriet Alexander[b], Andrew R. Juhl[a,c], Sonya T. Dyhrman[a,c,*]

[a] Columbia University, Lamont-Doherty Earth Observatory, Palisades, NY, USA
[b] Population Health and Reproduction, School of Veterinary Medicine, University of California, Davis, CA, USA
[c] Columbia University, Department of Earth and Environmental Sciences, Palisades, NY, USA

ARTICLE INFO

Article history:
Received 1 October 2016
Received in revised form 30 June 2017
Accepted 1 July 2017
Available online 6 September 2017

Keywords:
Heterosigma akashiwo
Harmful algal bloom
Phytoplankton
De novo assembly
Gene expression
Transcriptome

ABSTRACT

The marine eukaryotic alga *Heterosigma akashiwo* (Raphidophyceae) is known for forming ichthyotoxic harmful algal blooms (HABs). In the past 50 years, *H. akashiwo* blooms have increased, occurring globally in highly eutrophic coastal and estuarine systems. These systems often incur dramatic physicochemical changes, including macronutrient (nitrogen and phosphorus) enrichment and depletion, on short timescales. Here, *H. akashiwo* cultures grown under nutrient replete, low N and low P growth conditions were examined for changes in biochemical and physiological characteristics in concert with transcriptome sequencing to provide a mechanistic perspective on the metabolic processes involved in responding to N and P stress. There was a marked difference in the overall transcriptional pattern between low N and low P transcriptomes. Both nutrient stresses led to significant changes in the abundance of thousands of contigs related to a wide diversity of metabolic pathways, with limited overlap between the transcriptomic responses to low N and low P. Enriched contigs under low N included many related to nitrogen metabolism, acquisition, and transport. In addition, metabolic modules like photosynthesis and carbohydrate metabolism changed significantly under low N, coincident with treatment-specific changes in photosynthetic efficiency and particulate carbohydrate content. P-specific contigs responsible for P transport and organic P use were more enriched in the low P treatment than in the replete control and low N treatment. These results provide new insight into the genetic mechanisms that distinguish how this HAB species responds to these two common nutrient stresses, and the results can inform future field studies, linking transcriptional patterns to the physiological ecology of *H. akashiwo in situ*.

1. Introduction

The marine raphidophyte, *Heterosigma akashiwo,* forms harmful algal blooms (HAB) in coastal and estuarine systems worldwide (Honjo, 1992) and these blooms have increased in number and frequency over the past 50 years (Honjo, 1993; Anderson et al., 2008 and references therein). Many blooms of *H. akashiwo* have been reported to be ichthyotoxic, resulting in significant economic losses due to wild and farmed fish kills in coastal areas and estuaries of both the Atlantic and Pacific oceans (Chang et al., 1990; Honjo, 1993; Taylor and Haigh, 1993; Kempton et al., 2008; Rensel et al., 2010). Blooms of *H. akashiwo* have also been reported to have sublethal, adverse effects on the physiology of invertebrates, including oysters (Keppler et al., 2005) and zooplankton (Verity and Stoecker, 1982; Kamiyama, 1995; Kamiyama et al., 2000).

As a group, raphidophytes, including *H. akashiwo,* occupy a wide niche, as they are found in highly variable physicochemical coastal environments worldwide, including highly eutrophic systems with major macronutrient inputs from agricultural, industrial, and urban sources (Smayda, 1998; Zhang et al., 2006; Mohamed and Al-Shehri, 2012). Cells of *H. akashiwo* can vertically migrate on the order of 10–15 m on a diel cycle through highly temperature and salinity-stratified water (Smayda, 1998 and references therein) and nutrient retrieval by *H. akashiwo* migrating to more nutrient-rich depths has been documented (Watanabe et al., 1988). Thus, the motility of these cells may serve as a strategy to respond quickly to physicochemical disruptions, a trait that may be particularly useful in highly eutrophic systems that often incur rapid environmental change. Rapid environmental changes (even on the scale of days) may result from short nutrient residence times due to flushing or

* Corresponding author at: Department of Earth and Environmental Sciences and Lamont-Doherty Earth Observatory, Columbia University, Palisades, NY, 10964, USA.
E-mail address: sdyhrman@ldeo.columbia.edu (S.T. Dyhrman).

http://dx.doi.org/10.1016/j.hal.2017.07.001
1568-9883/

other physical processes, or as a result of rapid nutrient uptake by high biomass blooms followed by nutrient depletion (Glibert et al., 2010; Anderson et al., 2014). Migrations to acquire nutrients may be aided by this species' high affinity for nitrogen (N) and phosphorus (P). Studies have suggested that *H. akashiwo*, including strains isolated from highly-eutrophic systems, such as Delaware Inland Bays, has low half-saturation constants for these macronutrients, making it an effective competitor at low N and P levels (Zhang et al., 2006). In addition, *H. akashiwo* has been found to be mixotrophic, grazing heterotrophic bacteria and cyanobacteria to obtain N and P, which may enable, or enhance bloom development during periods of nutrient limitation (Nygaard and Tobeisen, 1993; Jeong et al., 2010, 2015).

Taken together, *H. akashiwo* employs multiple traits that facilitate bloom formation and maintenance in both high and low nutrient environments. Yet, the metabolic pathways that underpin its responses to high and low concentrations of N or P are largely unknown. Targeted molecular-based research on *H. akashiwo* is limited to the identification and transcriptional expression of nitrate reductases (NR), one of which has a unique active site that allows for the use of nitric oxide (NO) as a source of N (Coyne, 2010; Stewart and Coyne, 2011; Stewart, 2011). While this points to a novel strategy for N acquisition, even basic aspects of N and P acquisition strategies, and how they are regulated, have not been comprehensively examined in this species. Transcriptome profiling is increasingly used to identify N and P metabolic pathways in a global way that does not require prior knowledge of gene content (e.g., Koid et al., 2014; Liu et al., 2015a; Cooper et al., 2016). By comparing transcriptomes of cells grown under multiple conditions, this approach allows for identifying gene content as well as how those genes are regulated.

In this study, transcriptome profiling was used to examine gene content and expression patterns in toxic *H. akashiwo* strain CCMP 2393 with a focus on the response to nutrient depletion, a common source of stress for phytoplankton populations. Transcriptional patterns during growth under low N and low P conditions were compared to patterns under nutrient replete conditions to identify and compare the mechanistic responses that underpin shifts in *H. akashiwo* physiology in response to N and P stress.

2. Materials and methods

2.1. Culture conditions

Experiments were performed with *Heterosigma akashiwo* strain CCMP 2393 (isolated from Rehoboth Bay, Delaware, USA, September 2002) maintained on L1 medium (882 μM $NaNO_3$, 36.2 μM NaH_2PO_4, initial concentrations) made with a 0.2-μm filtered seawater base collected from Vineyard Sound, MA (salinity 32). The culture used was not axenic, but was uni-algal and uni-eukaryotic. Experiments were conducted at 18 °C on a 14:10 light:dark cycle provided by cool-white fluorescent lights at an intensity of approximately 100 μmole photons $m^{-2}\,s^{-1}$ of photosynthetically-active radiation (400–700 nm).

2.2. Experimental design

Entrainment cultures were used to initiate experimental cultures to decrease carryover of nutrients from stock cultures and promote acclimation to the experimental conditions. Single entrainment cultures (~ 100 mL) were grown in modified L1 medium (base water as above) under the following culture conditions: low P (0.2 μM NaH_2PO_4), low N (5 μM $NaNO_3$), and a nutrient-replete control culture with initial N:P adjusted to 16:1 (576 μM $NaNO_3$ and 36.2 μM NaH_2PO_4). Entrainment cultures were kept at 18 °C on a 14:10 light:dark cycle (as above) with gentle rotation (75 rpm) for 3 days. Experiments were initiated by inoculating triplicate 1-L bottles for each treatment (low P, low N, and replete) with 25 mL of the corresponding entrainment culture and maintaining the replicate bottles under the same conditions as the entrainment cultures. Growth in each bottle was monitored by in vivo chlorophyll fluorescence on a Turner Designs TD-700 fluorometer. Samples were also collected for cell counts and photosynthetic efficiency (F_v/F_m). Measurements were made at the same time each day (during the middle of the light phase) to avoid diel changes in gene expression and cell physiology. The nutrient-replete control was harvested during exponential phase growth and the treatments were harvested once growth rates and cell yields were reduced relative to the replete control (Table 1, See Supplementary files: Fig. S1 in the online version at doi:10.1016/j.hal.2017.07.001). This sampling scheme allowed for the identification of N and P effects independently, and a similar approach has been used for previous gene expression studies (e.g., Dyhrman et al., 2006, 2012; Wurch et al., 2011a, 2011b; Bender et al., 2014). A growth experiment of similar design was repeated for the replete and low P treatments to assay how alkaline phosphatase activity (APA) changed in the low P treatment relative to the replete control.

2.3. Culture analysis and biochemical measurements

Cell count samples were preserved in 2% (final concentration) acid Lugol's solution and cell concentrations were determined by microscopic counts. The efficiency of photosystem II (PSII), F_v/F_m, was determined from each replicate at initiation (T = 0) and harvest (T = final) of the experiment using the DCMU (3,4-dichlorophenyl-1,1-dimethylurea) method (Parkhill et al., 2001). Briefly, 5 mL subsamples were kept in the dark for 30 min (at 18 °C) before measuring F_0 on a Turner Designs TD-700 fluorometer. Photosynthesis was inhibited with the addition of 2.5 μL 30 mM DCMU (in 100% ethanol) to a final concentration of 15 μM and maximum fluorescence (F_m) was measured after 30 s. All readings were blank corrected, and F_v/F_m was calculated as: $F_v/F_m = (F_m - F_0)/F_m$. Additional measurements, including in vitro chlorophyll *a* concentration (chl *a*), POC/PON, and particulate carbohydrate (pCHO) concentration, were taken at the time of harvest from each replicate. For chl *a* determination, 10 mL was filtered through a Whatman GF/F (25 mm) and stored at −20 °C prior to extraction. Chlorophyll *a* was extracted in 10 mL 90% acetone, vortexed for 15 s at maximum speed, and stored in the dark at −20 °C for 12 h. After extraction, each sample was centrifuged. Chlorophyll *a* concentration was determined from fluorescence of the supernatant before and after acidification (Strickland and Parsons, 1972) using a Turner Designs Aquafluor fluorometer. The fluorometer was calibrated using chl *a* from *Anacystis nidulans* algae (Sigma). For pCHO measurements, 25 mL was filtered onto pre-combusted Whatman GF/F (25 mm) and stored at −20 °C prior to analysis by a modified phenol-sulfuric acid method (Dubois et al., 1956). Briefly, filters were soaked in 5% phenol and concentrated sulfuric acid in the original sample tubes at 30 °C. The filter was then removed, and light absorption of the sample at 490 nm was measured using a Hach DR2700 spectrophotometer and compared to a glucose standard curve. Results are reported as glucose equivalents. Total POC/PON (50 mL) were filtered through pre-combusted (450 °C for 5 h) Whatman GF/F filters (25 mm) and stored in pre-combusted foil packets at −20 °C. Samples were analyzed by the Nutrient Analytical Services Laboratory at the Chesapeake Bay Laboratory (University of Maryland, Solomons, MD) on a CE-440 Elemental Analyzer following the methods of USEPA (1997) for POC/PON. All results of the measurements listed were normalized to the cell concentrations in their respective flask. These cell-specific values were used for statistical comparisons. Prior to analysis,

homogeneity of variance was confirmed by the Brown-Forsythe test. Results were analyzed statistically using one-way ANOVAs followed by Fisher's least significant difference (LSD) post hoc tests to determine whether the means of the low N and low P samples were significantly different from the replete samples.

Alkaline phosphatase activity (APA) was assayed from triplicate biological samples from a repeated replete and low P experiment. Samples (25 mL) were filtered onto 47 mm polycarbonate membranes (0.2 μm) and stored at −20 °C until analysis. Activity was assayed after Dyhrman and Ruttenberg (2006) using the fluorogenic phosphatase substrate 6,8-difluoro-4-methylumbelliferyl phosphate. Cell-specific APA in the two treatments were compared using an unpaired *t* test.

2.4. Total RNA extraction and sequencing

At the time of harvest, triplicate 150 mL subsamples of each replicate in each treatment were filtered onto polycarbonate filters (47 mm, 3 μm). The filters were immediately flash frozen and stored in liquid nitrogen. All RNA extractions were performed with the RNeasy Mini Kit (Qiagen, Valencia, CA) with a small modification to the lysis procedure. Lysis was performed by adding 1.4 mL Buffer RLT and ∼250 μL zirconium/silica beads (0.5 mm) and vortexing for 1 min at 250 rpm. The RNA was then treated with TurboDNase (Ambion, Austin, TX) following the standard protocol to remove genomic DNA. Extracts from triplicate cultures of each experimental condition were pooled prior to sequencing to average across biological variability in transcriptional response between replicate flasks, as has been done in other studies (Frischkorn et al., 2014; Dyhrman et al., 2012). Total RNA of samples was quantified using a Qubit fluorometer (Invitrogen, Carlsbad, CA) and RNA quality was assessed using the Agilent 2100 Bioanalyzer (Agilent, Santa Clara, CA). The Illumina TruSeq RNA Sample Preparation Kit was used by the National Center for Genome Resources (NCGR, Santa Fe, NM) to generate libraries using ∼2 μg of RNA. Sequencing of 50 base pair paired-end reads from each library was performed on an Illumina HiSeq 2000 at the NCGR.

2.4.1. Transcriptome assembly and annotation

A combined assembly was generated by NCGR from reads from single assemblies (replete, low N, and low P) as part of the Marine Microbial Eukaryote Transcriptome Sequencing Project (MMETSP) (Keeling et al., 2014) using their internal pipeline called BPA2.0 (Batch Parallel Assembly version 2.0). Sequence reads were preprocessed using the SGA preprocess (Simpson and Durbin, 2012) for quality trimming (swinging average) at Q15. Reads less than 25 bp after trimming were discarded. Preprocessed sequence reads from each sample were assembled into contigs with ABySS (Simpson et al., 2009). A minimum kmer coverage of 5 was used, with popping at >0.9 branch identity, and with the scaffolding flag disabled to avoid over reduction of divergent regions. Unitigs from all kmer assemblies and all samples were combined and redundancies were removed using CD-HIT-EST (Li and Godzik, 2006) with a clustering threshold of 98% identity. The overlap layout consensus (OLC) assembler CAP3 (Huang, 1999) was used to identify minimum 100 bp overlaps between the resultant contigs and assemble larger sequences. The resulting contigs were paired-end scaffolded using ABySS (Simpson et al., 2009). Sequence read pairing information was used in GapCloser (v. 1.10) from SOAP *de novo* assembly software (Li et al., 2008) to walk in on gaps created during scaffolding. Redundant sequences were again removed using CD-HIT-EST at a clustering threshold of 98% identity. In an attempt to remove incomplete sequences, the consensus contigs were filtered at a minimum length of 150 bp to produce the final set of contigs. Sequence data for the *H. akashiwo* (CCMP2393) combined assembly is available on *i*Microbe (http://data.imicrobe.us/combined_assembly/view/47) with the identification numbers MMETSP0292 (replete), MMETSP0294 (low N), and MMETSP0295 (low P).

Initial annotations were derived through the MMETSP annotation bundle, where hits against the UniProtKB and Swiss-Prot databases were determined using BLASTp (Altschul et al., 1990) and identified coding sequences were further characterized with Pfam-A, TIGRFAM, and SUPERFAMILY databases using HMMER3 (Haft et al., 2001; Gough et al., 2001; Zhang and Wood, 2003; Bateman, 2004). A second annotation effort identified biochemical pathways for each contig using the Kyoto Encyclopedia of Genes and Genomes (KEGG) database using the partial genome single-directional best-hit method (Kanehisa, 2006). In addition, orthologous genes were clustered using the Identification of Ortholog Groups for Eukaryotic Genomes (OrthoMCL) software and default settings (Li et al., 2003). The annotations of the transcripts presented herein are putative (Supplementary files: Table S1 and Fig. S1 in the online version at doi:10.1016/j.hal.2017.07.001). Roughly 70% of contigs were unannotated (Supplemental Fig. 2). This is consistent with other studies of phytoplankton, where 50–60% of the contigs in the assembled transcriptomes remained unannotated (Frischkorn et al., 2014; Cooper et al., 2016).

Counts for each contig were quantified by first using Bowtie2 run with the "–sensitive" parameters in "–end-to-end" mode in order to align trimmed reads to the final contigs produced by the ABySS assembly. These Bowtie2 settings were chosen because previous studies have shown that increasing the sensitivity does not yield a dramatic increase in the percentage of reads aligned but does greatly increase computation time (Langmead and Salzberg, 2012) and because Bowtie2 alignments have been shown to be less sensitive to altered parameters than similar alignment programs (Lindner and Friedel, 2012). The HTSeq Count program was then used to obtain transcript abundance (Anders et al., 2014).

2.4.2. Differential contig abundance analysis

Significant changes in the relative abundance of contigs derived from pooled biological replicates in the low N and low P treatments versus the replete (control) condition were assigned using the Analysis of Sequence Counts (ASC) method, using a posterior probability (post-*p*) of 0.95 for a fold change >2 (Wu et al., 2010. Thus, a given contig is considered significant when there is 95% confidence that the fold change (relative to the control) was >2, setting significance consistent with other studies of this type with eukaryotic algae (Dyhrman et al., 2012). The ASC method is an empirical Bayes approach that estimates the prior distribution of difference between conditions by modeling biological variability using the large number of sequences quantified within an experiment, rather than imposing a negative binomial distribution. Thus, differential contig abundance is assigned based on the posterior expectation of log fold change. This biologically-averaged approach has been shown to perform similarly, but conservatively, relative to other differential abundance analyses implemented on data sets with and without replicates (Wu et al., 2010; Biswas et al., 2013). This method has been applied successfully in a number of studies for which sequenced replicates were not available (Thomas et al., 2012; Konotchick et al., 2013; Huang et al., 2015; Kopf et al., 2015; Spungin et al., 2016) and in studies for which sequenced replicates were not tractable, but biological replicates were pooled prior to sequencing (Alexander et al., 2015b and references therein). For simplicity, the ASC statistics denoting a significant difference in relative contig abundance (i. e., post-$p > 0.95$, fold change > 2), are abbreviated "ASC" from this point forward.

In addition to examining differential abundance at the single contig level, enrichment patterns were investigated for contigs grouped into gene sets, groups of genes defined based on prior

biological knowledge (e.g., metabolic pathways, protein families, or related biological function) (Subramanian et al., 2005). First, within each *a priori* defined gene set, the TPM per contig in each treatment were normalized to the average abundance of that contig across the three treatments (replete, low N and low P). This normalization step was necessary to equalize the relative contribution of each contig to the gene set, thereby avoiding bias from having contigs within the gene set with different inherent levels of abundance. This resulted in three distributions of normalized enrichments of contigs within the gene set, one distribution for each treatment. These distributions were then compared using Kolmogorov-Smirnov tests, with significance at $p < 0.05$, to examine the null hypothesis that normalized enrichments (within a gene set) in the low N and low P treatments had the same distribution across contigs as the replete control. Thus, rejecting the null hypothesis for a treatment indicated a significantly different pattern of normalized contig abundance within the specified gene set compared to the replete control. Because the test does not specify how the distributions differ, when gene sets are described as significantly enriched (or significantly less abundant) relative to the control, the description implies a significant test result, combined with a consistent direction of differential abundance across contigs within the gene set, a direction apparent in plots of the distributions. Kolmogorov-Smirnov tests used Prism (GraphPad Software, La Jolla, CA), which uses a boot-strapping approach to calculate exact *p*-values for 2-sample Kolmogorov-Smirnov tests.

3. Results and discussion

The raphidophyte *H. akashiwo* has been forecasted to be an important constituent in a shifting coastal ocean environment (Smayda, 1990). Coastal systems experience rapid changes in nutrient inputs via natural changes and variability in freshwater inputs and tidal flushing, and increased anthropogenic activities are altering nutrient ratios in these zones (Voss et al., 2011; Glibert et al., 2015), which may drive phytoplankton populations to more frequent N or P stress. Herein physiological and transcriptional patterns associated with growth on low N or low P were compared to a replete control and to each other.

3.1. Cellular physiology

The replete cultures were harvested during the exponential phase of growth, while the low N and low P cultures were harvested when growth rates and yields dropped relative to the replete cultures, indicating the onset of nutrient stress (See Supplementary Fig. S1 in the online version at doi:10.1016/j.hal.2017.07.001). At the time of harvesting, the physiology of cells in the low N and low P treatments was significantly different from the replete cultures with respect to several variables. Mean growth rate of the replete cultures (0.47 d^{-1}) was consistent with expectations for the light level and temperature (Zhang et al., 2006) and significantly higher than those of the low N and low P treatments (0.36 and 0.37 d^{-1} respectively) (Table 1). In addition, both low-nutrient treatments had significantly lower mean photosynthetic efficiency of photosystem II (F_v/F_m) (Table 1). There was also a significant increase in both particulate carbohydrates and C:N under both low-nutrient conditions compared to the replete control, with a more robust response for both parameters observed under low N ($p < 0.0005$) (Table 1). Although growth rates and photosynthetic efficiency of the low-nutrient cultures declined, other physiological indicators (such as chl *a* $cell^{-1}$) were not significantly affected, indicating that the treatment cultures were nutrient-stressed, closer to nutrient limitation, rather than nutrient starvation (*sensu* MacIntyre and Cullen, 2005) at the time of harvest. Treatments will be referred to as stressed throughout.

Table 1
Cellular elemental composition, particulate carbohydrate and chlorophyll *a* (chl *a*) concentrations, growth rate, F_v/F_m, and RNA at the point of harvest.

	Replete	-N	-P
Growth rate (d^{-1})	0.47 (12%)	0.36 (2%)*	0.37 (12%)*
F_v/F_m	0.70 (2%)	0.61 (1%)****	0.66 (0.2%)**
Chl *a* ($\mu g\,cell^{-1}$)	6.39E-06 (16%)	6.75E-06 (23%)	4.91E-06 (3%)
pCHO ($pmoles\,cell^{-1}$)	5.54 (6%)	45.85 (13%)****	15.57 (35%)*
RNA ($pg\,cell^{-1}$)	19.22 (21%)	12.25 (22%)*	1.27 (23%)***
POC ($pmoles\,cell^{-1}$)	24.83 (19%)	73.47 (20%)	36.74 (22%)
PON ($pmoles\,cell^{-1}$)	3.86 (17%)	5.12 (20%)**	4.14 (26%)
C:N	6.42 (2%)	14.37 (7%)****	8.95 (8%)**

Values represent the mean (n = 3) with coefficient of variation (CV), the ratio of standard deviation to the mean, in parentheses. Asterisks indicate significantly different from replete, where one asterisk is $p < 0.05$, two asterisks are $p < 0.005$, three asterisks are $p < 0.0005$ and four asterisks are $p < 0.0001$, using one-way ANOVA with Fisher's LSD post-hoc test. Elemental ratios are molar.

3.2. Global transcriptional response

The combined ABySS assembly yielded 40,801 contigs (Table 2). Of these, 14,013 contigs were significantly differentially abundant (ASC) (Wu et al., 2010; Dyhrman et al., 2012) across both low nutrient treatments, resulting in 31% and 16% differentially abundant contigs in the low N and low P treatments, respectively (Fig. 1, See Supplementary Figs. S2 and S3 in the online version at doi:10.1016/j.hal.2017.07.001). These percentages are consistent with the levels of differentially modulated contigs in other transcriptome studies of eukaryotic phytoplankton, such as *Prymnesium parvum* grown under low N and low P conditions (Liu et al., 2015a), although higher than what has been reported in dinoflagellates (11–12%, e.g., Morey et al., 2011). The general stress response, where the same contig was differentially abundant in both the low N and low P treatments relative to the control, constituted about ~30% (4133 contigs) of the total differential response (Fig. 1). The low N treatment had more unique contigs that were significantly differentially abundant (Fig. 1), than the low P treatment, in addition to a greater number of contigs with fold change > 4 (Fig. 1), resulting in a broader (more contigs) and stronger (higher fold changes) response to N stress relative to P stress. This same pattern was observed when the contigs were examined at the orthologous group level (Supplemental Fig. S3). It is possible that the differences in transcriptional pattern between the low N and low P transcriptomes reflect a general difference in cellular responses to N and P stress. This pattern of a broader and stronger transcriptomic response to N stress compared to P stress has also been observed in other phytoplankton, including *Microcystis aeruginosa* (Harke and Gobler, 2013) and *Karenia brevis* (Morey et al., 2011) and in higher plants, including rice and *Arabidopsis* (Cai et al., 2012a, 2012b, and references therein). However, it is also possible that these differences are related to growth phase, or the relative degree of stress in the respective treatments. Even though growth rates were nearly equally depressed relative to the controls in the low nutrient treatments, the degree of stress on the cells in the experiments is difficult to quantify, and a more dramatic transcriptional response might have developed in the low P treatment if the P stress became more severe. For example, Johnson et al. (2012) demonstrated sequential changes in transcript abundance as the growth rates declined in cultures of the dinoflagellate *Karenia brevis*. Moreover, bacterivory, which may serve as a strategy to acquire N or P, was not constrained here since the cultures were not axenic. Switching between nutritional modes may influence

Table 2
Summary of ABySS combined assembly statistics for *Heterosigma akashiwo*.

Sequences/contigs	Number of characters	Max Length	Min Length	N50	Sample identifiers	Read counts
40801	35668425	13907	150	1402	MMETSP0292 (Replete)	32,622,070
					MMETSP0294 (Low N)	31,175,731
					MMETSP0295 (Low P)	23,209,198

transcriptional patterns in the N or low P treatments. Regardless, *H. akashiwo* clearly exhibits a robust global transcriptional response to changes in the nutrient environment in culture, with marked differences between the responses to low N and low P.

To examine transcriptional differences further, contigs were annotated using KEGG orthology. At the module level (e.g., carbohydrate and lipid metabolism, energy metabolism, etc), there was a broad metabolic response to both low N and low P conditions (Fig. 2). Because many contigs are pooled within each module, changes in expression of modules are less extreme than at the individual contig level (e.g., Fig. 1). However, as described above, the overall pattern of the responses was different between low N and low P, with larger changes to more modules under low N (Fig. 2). Within the low N transcriptome, the abundance changes within some modules were related to a high representation of genes for N assimilation, transport, or metabolism. For example, the KEGG N metabolism module was significantly enriched under low N when compared to the replete control (Kolmogorov-Smirnov test, $p < 0.0001$) (Figs. 2,3A). In addition to the N metabolism module, other modules that responded in the low N treatment included the photosynthesis and glycosaminoglycan metabolism modules, which declined and increased, respectively, under low N (Fig. 2), and were connected to phenotypic changes observed in this study. A KEGG P metabolism module comparable to the N metabolism module does not exist, though effects of P stress on other modules are described below.

In the photosynthesis KEGG module, which includes photosystem proteins (Fig. 2, See Supplementary Table S1 in the online version at doi:10.1016/j.hal.2017.07.001), there was significantly lower abundance in the low N and low P treatments (Kolmogorov-Smirnov test, $p = 0.0007$ and $p = 0.0063$, respectively) relative to the replete control (Fig. 3B) with the greatest decline under low N. Coincident with these changes, photosynthetic efficiency (F_v/F_m) was significantly lower under low N (0.61) and low P (0.66) compared to the replete control (0.70) (Table 1). Similar findings have been reported for other phytoplankton groups, including dinoflagellates (*Scrippsiella trochoidea*), prymnesiophytes (*Prymnesium parvum*), haptophytes (*Emiliania huxleyi*), and pelagophytes (*Aureococcus anophagefferens*), where genes involved in photosystem I and II light-harvesting complexes were significantly less abundant under low N conditions (Dyhrman

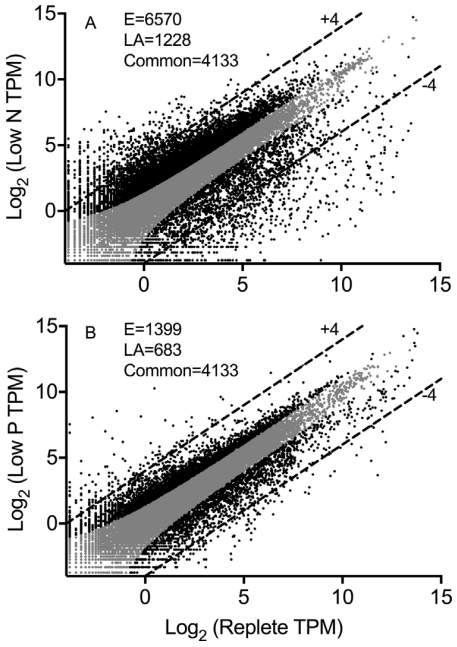

Fig. 1. Pairwise comparison of transcriptional responses across 40,801 contigs in each treatment (low N, panel A, and low P, panel B) relative to the replete control. Contigs were normalized to total library size in tags per million (TPM). Grey points represent contigs that were not significantly differentially abundant. Significance (Black points) was determined with ASC (post-$p > 0.95$ and fold change > 2) (Wu et al., 2010). Dashed lines indicate four-fold change (up and down) relative to the replete control to facilitate pattern recognition. Inset lists the number of unique contigs significantly enriched (E), significantly less abundant (LA), significantly differentially abundant in both low N and low P (Common).

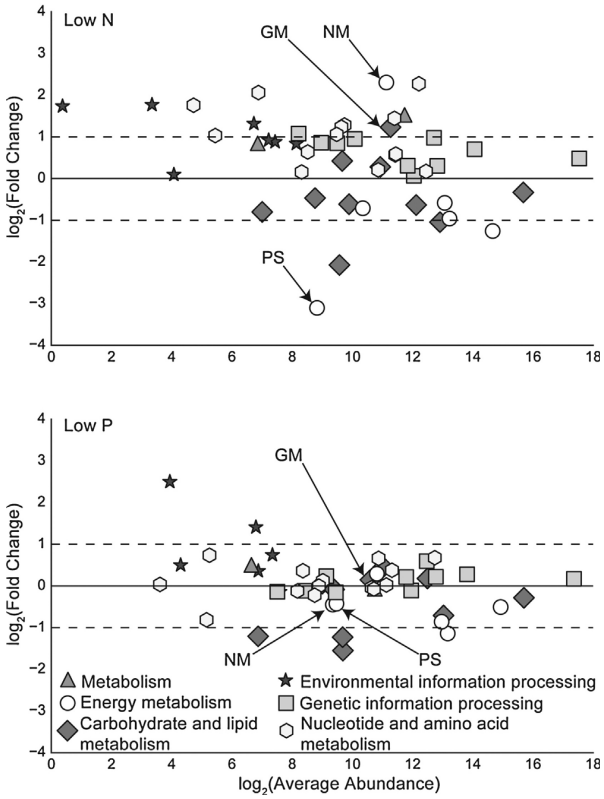

Fig. 2. Fold change plots for global shifts in expression of KEGG orthologs. Fold change (log2) and average read count abundance (log2) are plotted for low N and low P, where the replete is represented with a solid line. KEGG modules are indicated with different symbols. GM, Glycosaminoglycan metabolism; NM, Nitrogen metabolism; PS, Photosynthesis. Dashed lines bin KEGG modules at +1 and −1 fold change to facilitate pattern identification. They do not indicate significance. Symbol key indicates KEGG functional categories.

et al., 2006; Frischkorn et al., 2014; Liu et al., 2015; Cooper et al., 2016).

The glycosaminoglycan KEGG module was significantly enriched in both low nutrient treatments (Fig. 2, Fig. 3C). Most of the contigs within the module were enriched under low N (Kolmogorov-Smirnov test, $p < 0.0001$). Changes in enrichment under low P were less consistent across contigs, though the overall distribution was significantly different from that of the replete treatment (Kolmogorov-Smirnov test, $p < 0.005$). Glycosaminoglycans (GAGs) are large, complex carbohydrates, often referred to as mucopolysaccharides. They can be involved in a suite of physiological processes, including cell adhesion and cell growth and differentiation (Gandhi and Mancera, 2008). The shifts in transcription can be connected to phenotypic observations in the cultures, where particulate carbohydrates (pCHO) concentrations were significantly increased in low N (45.85 pmoles/cell) and low P (15.57 pmoles/cell) compared to the control (5.54 pmoles/cell), though to a much greater extent under low N (Table 1). These changes in pCHO also contributed to the significant differences observed in C:N ratios of the cultures, illuminating some of the metabolic processes that may contribute to variable C:N ratios in phytoplankton. Within the glycosaminoglycan KEGG module, many of the most enriched contigs (as determined by ASC) under low N were annotated as sulfatases or sulfotransferases. Sulfated forms of polysaccharides, with GAG-like properties, have been found in both marine eukaryotes and prokaryotes (Senni et al., 2011), and it is well documented that a variety of marine microalgae, including dinoflagellates, diatoms, pelagophytes and raphidophytes, produce sulfated extracellular polysaccharides (EPS) (Gobler et al., 2011; Lopes et al., 2012; De Jesus Raposo et al., 2013) that have a high carbohydrate content. The change in contig abundance for the sulfatases and sulfotransferases suggests that *H. akashiwo* may systematically remodel and biosynthesize glycosaminoglycans in response to a decrease in N availability. Because they contain N, reprocessing of GAGs could serve to acquire N from internal or extracellular reservoirs. In addition, the generation of EPS or other GAGs may also mediate the process of cell adhesion and aggregation, facilitating the transmission of allelopathic compounds, particularly through direct cell-cell interactions (Lopes et al., 2012). Aggregation mediated by increased EPS production could also increase sinking rates (Engel, 2000; Engel et al., 2014), which might be advantageous if deeper waters have higher nutrient concentrations. Finally, mucus production by *H. akashiwo* has been shown to play a role in mixotrophy (Jeong, 2011), and implicated as a possible mechanism for fish-kills associated with its blooms (Smayda, 1998, and references therein). Given their potential role in toxicity and physiological ecology, these observations collectively suggest that carbohydrate metabolism, and glycosaminoglycan metabolism specifically, should be examined in greater detail in both cultured and field populations of harmful raphidophytes.

3.2.1. General patterns of differential abundance

An examination of the 10 contigs with the greatest fold change in *H. akashiwo* under low N and low P compared to the replete control revealed several trends. Of the top 10 contigs with increased relative abundance under low P, 50% were annotated as phosphate transporters or phosphatases. Of the 10 contigs that decreased under low N, eight encoded genes involved in chlorophyll a/b binding (See Supplementary Table S2 in the online version at doi:10.1016/j.hal.2017.07.001). This is consistent with the lower abundance of the photosynthesis KEGG module under low N (Fig. 2). The 10 contigs with increased relative abundance under low N included several (40%) related to amino acid metabolism as well as genes whose relation to N metabolism is unclear (Supplemental Table S2). In the low P transcriptome, half of the 10 contigs that decreased were related to carbon fixation (e.g., fructose-1-6-bisphosphate aldolase and fructose-1-6-bisphosphatase). While there was no overlap in the annotations of this subset of contigs within the low N and low P transcriptomes, there was some similarity in that many of the genes that decreased in both conditions were related to carbon fixation and photosynthesis. Conversely, many of the genes that were

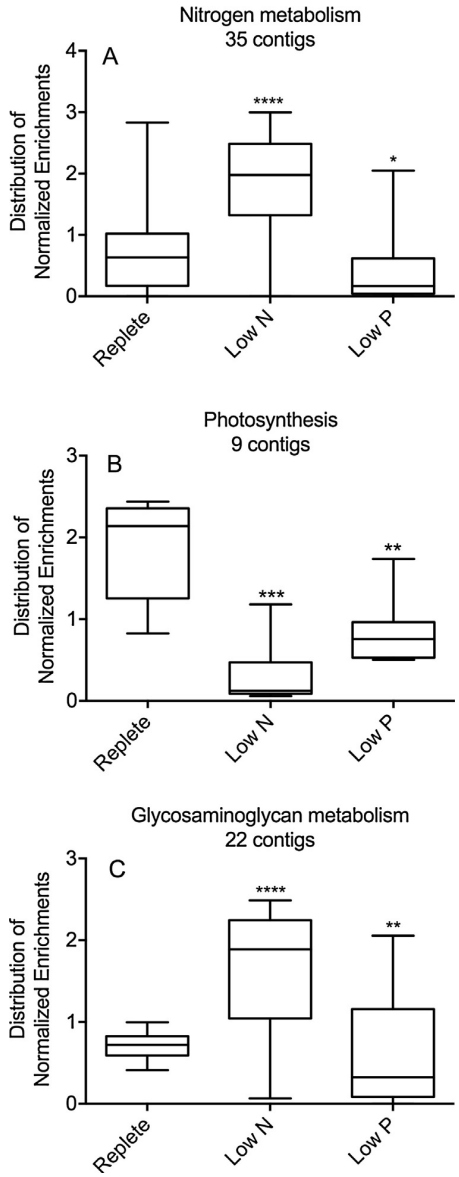

Fig. 3. Distribution of normalized enrichments for N-related (A) KEGG pathways and for pathways with coincident changes observed in photosynthetic efficiency (B) and carbohydrate metabolism (C). Distributions were compared using Kolmogorov-Smirnov tests. Whiskers show the normalized enrichment level for the least enriched, and most enriched contigs for each treatment within the module. Boxes encompass the normalized enrichment levels for the upper and lower 25th percentiles of contigs for each treatment within the module. The horizontal lines show the median normalized enrichment of contigs for each treatment within the module. Significance is indicated with asterisks, where one asterisk is $p < 0.05$, two asterisks are $p < 0.005$, three asterisks are $p < 0.0005$ and four asterisks are $p < 0.0001$.

enriched in each treatment were related to metabolism of the limiting nutrient.

3.2.2. Differential abundance of N-specific genes

The *H. akashiwo* low N response was characterized by the modulation of contigs encoding genes involved in uptake and assimilation, including ammonium and nitrate transporters, nitrate reductase, and the uptake and processing of urea. Individual contigs were tested for significant differential abundance using ASC, and then *a priori* defined 'gene sets' based on gene families, or metabolic pathways were examined using Kolmogorov-Smirnov tests to assess whether the pattern of contig abundance was significantly different from that of the replete control.

Twenty contigs annotated as ammonium transporters were identified, falling into the same orthologous group (See Supplementary Table S1 in the online version at doi:10.1016/j.hal.2017.07.001), and the majority of the individual contigs were significantly enriched under low N compared to the replete control (ASC) (Table 3). The gene set as a whole was also significantly enriched under low N compared to the replete control (Kolmogorov-Smirnov test, $p < 0.0001$) (Fig. 4A), while there was no significant difference in the distribution of enrichments across ammonium transporters under low P. Nitrate transporters, at the contig level, were predominantly found to be significantly enriched under low N (ASC) (Table 3). Similarly, the gene set was significantly enriched under low N (Kolmogorov-Smirnov test, $p = 0.0025$), while significantly less abundant under low P (Fig. 4B). This pattern of enhanced NO_3^- or NH_4^+ transporter expression under low N has been observed for other groups of phytoplankton, including diatoms (Dyhrman et al., 2012; Bender et al., 2014), pelagophytes (Berg et al., 2008; Wurch et al., 2011a; Frischkorn et al., 2014, 2015a), and dinoflagellates (Morey et al., 2011), suggesting that this is a conserved aspect of the N stress response in marine phytoplankton. The same trend was observed for contigs annotated as nitrite/formate transporters where several of the individual contigs were significantly enriched under low N (ASC), although the trend was not significant across the gene set using the Kolmogorov-Smirnov test ($p = 0.10$) (Table 3). This response has also been observed in other HAB species like *A. anophagefferens* (Berg et al., 2008; Wurch et al., 2011a; Frischkorn et al., 2014). Nitrogen preference, based on uptake kinetics, suggests *H. akashiwo* has a preference for $NH_4^+ > NO_3^-$ (Herndon and Cochlan, 2007), which is likely mediated by changes in abundance of the transporters observed here. Although inorganic N transporters are typically enriched by N stress, they can also in some cases be substrate responsive (Glibert et al., 2015 and references therein), so future work might focus on how this suite of N transporters is modulated by growth of *H. akashiwo* on different N sources.

In addition to contigs involved in N transport, multiple contigs involved in nitrogen metabolism were found, including nitrate reductase (NR), glutamine synthetase (GSII) and glutamate

Table 3
Differential abundance of N-related contigs discussed in this study.

Functional Annotation	Contig IDs
Nitrate transporter	**3756, 10130, 10175, 13857**, 22339, 32001, **38230, 40313**
Ammonium transporter	**5930, 6548, 6679, 6860, 12462, 13124,** 18996**, 23605, 24345, 27471, 28652,** 30198, 32964, 33712, **38126, 38608, 38880,** *39388*, **39591, 40519**
Nitrite/formate transporter[a]	**19895,** 30087, **33417**
Nitrate reductase	1880, 2797, *2804*, 3080, 3599, 6377, **7359**, *15142*, *16208*, 18930, 19730, **19854**, **20376**, *21489*, **21738**, 22241, 22328, 28534, 29821, **31343,** *31594*, *31652*, **31741, 33163, 33648, 35303**, *36544*,*36553, 37199,* 37910, **38720,** 39251, 40076, 40091
Glutamine synthetase (GS2)	7853, **37583**
Glutamate synthase (GLT)	1057, **8143, 10532**
Carbamoyl phosphate synthase (CPS3)	**10007, 15400, 20726, 23666,** 30509, 30855, **33591**
Ornithine carbamoyl transferase	12500, 36044, 38881
Argininosuccinate synthase	**26709**
Argininosuccinate lyase	4472, **37479**
Urea transporter (DUR3)	**3206, 7502,** 29292, 30623
Urease (UreA,C) and accessory proteins	1269 (UreC), **9932** (UreD), 17091 (UreG), 17261 (UreA)

Contig IDs listed in bold were significantly enriched and those listed in italics were significantly less abundant under low N as determined by ASC (post-$p > 0.95$ and fold change > 2). Underlined contig IDs have putative homology to *H. akashiwo* NR2-2/2HbN. Change in shading (light to dark grey) indicates gene sets presented in Fig. 4.

[a]This variability in abundance yielded a distribution of normalized enrichment for this gene set that trended toward higher enrichment under low N, although the trend was not significant (Kolmogorov-Smirnov test, $p = 0.10$)

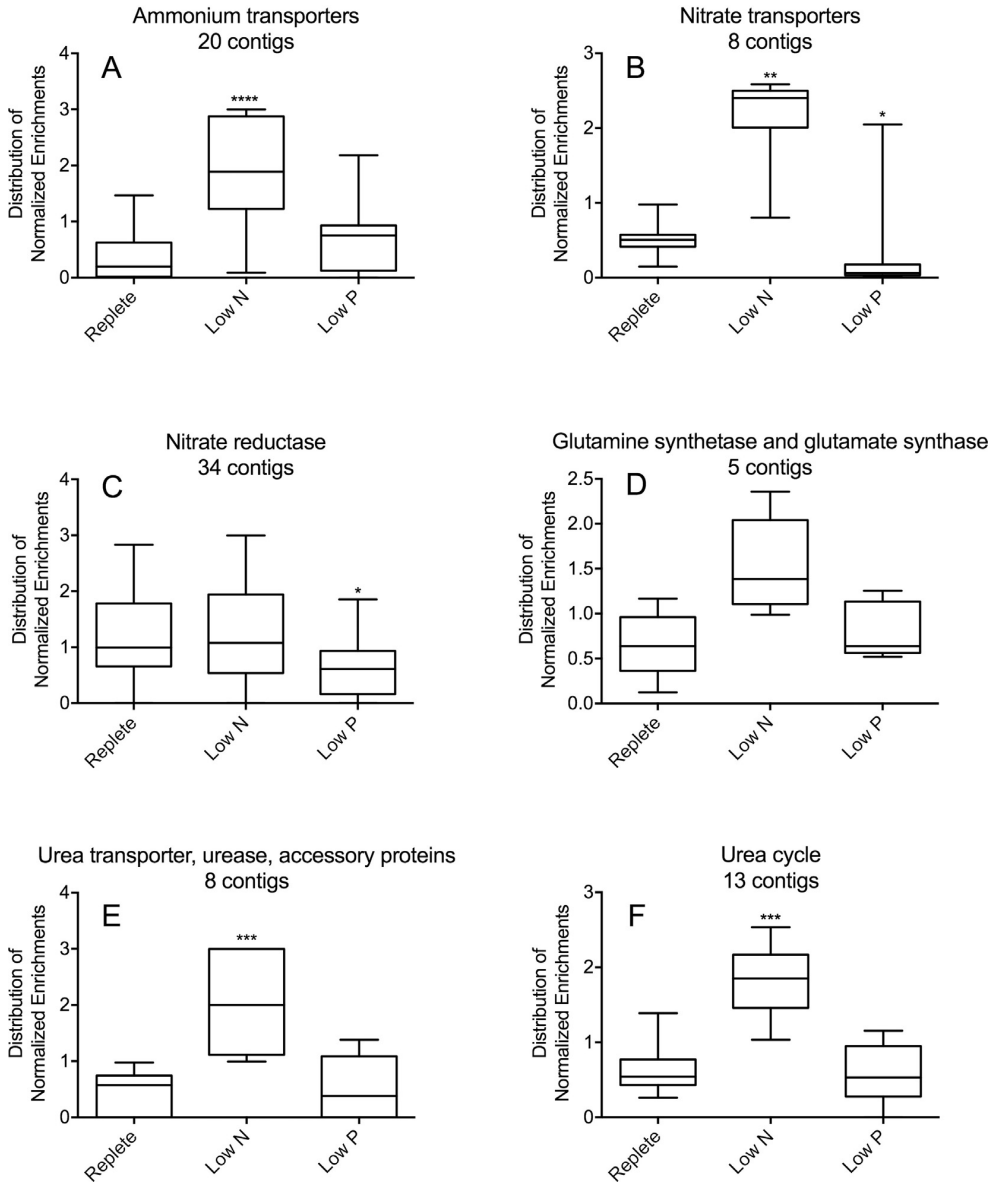

Fig. 4. Distribution of normalized enrichments for N-related gene sets, A) ammonium transporters, B) nitrate transporters, C) nitrate reductase, D) glutamine synthetase and glutamate synthase, E) urea transporter, urease and accessory proteins, and F) urea cycle. Distributions were compared using Kolmogorov-Smirnov tests. Whiskers show the normalized enrichment level for the least enriched, and most enriched contigs for each treatment within the gene set. Boxes encompass the normalized enrichment levels for the upper and lower 25th percentiles of contigs for each treatment within the module. The horizontal lines show the median normalized enrichment of contigs for each treatment within the module. Significance is indicated with asterisks, where one asterisk is $p < 0.05$, two asterisks are $p < 0.005$, three asterisks are $p < 0.0005$ and four asterisks are $p < 0.0001$.

synthase (GLT). Although many contigs were annotated as putative nitrate reductases in the *H. akashiwo* transcriptomes, their differential abundance was variable (Table 3), and the gene set was not significantly different under low N compared to the replete control (Kolmogorov-Smirnov test, $p = 0.97$) (Fig. 4C). Nitrate reductase enzyme activity and gene transcription is thought to be influenced by light availability and source of N in *H. akashiwo* (Smith et al., 1992; Berges, 1997; Liu et al., 2015b), although Coyne (2010) reported NR expression (as NR1) to be constitutive in *H. akashiwo* grown with and without N and in the presence of ammonium. As Coyne (2010) suggests, constitutive expression of NR in *H. akashiwo* could confer a unique competitive advantage over other phytoplankton species, particularly in estuaries with rapid nutrient fluctuations and diverse nutrient sources. The large number of NR contigs in *H. akashiwo*, and their inconsistent regulation, may relate to apparent discrepancies in earlier research. In addition, the disparate observations relating to the response of NR to both N limitation and N source in other microalgae (Eppley et al., 1969; Kessler and Osterheld, 1970; Berges et al., 1995; Coyne, 2010 and references therein) suggests that other organisms may share this characteristic.

As an example of the diversity found within NRs, a hybrid NR was recently identified in two raphidophytes, *H. akashiwo* and *Chattonella subsalsa*. This hybrid NR (NR2-2/2HbN) has a 2/2

hemoglobin (2/2Hb) inserted into the hinge 2 region of NR1, which, in some bacteria, confers the ability to convert nitric oxide to nitrate (Stewart and Coyne, 2011). The expression of this form of NR has been found to increase in response to nitric oxide addition, thereby serving as a means of metabolizing NO as a precursor to biologically available nitrate (Stewart and Coyne, 2011). A survey of the transcriptomes presented in this study revealed several contigs in the low N transcriptome (tblastx, e-value > 1e-5) homologous to the NR2-2/2HbN nitrate reductase hybrid identified in *H. akashiwo* (Table 3). The abundance of these contigs was variable, although the sequence producing the best alignment (20376) was significantly enriched under low N (as determined by ASC) (Table 3).

The GS-GOGAT cycle is responsible for assimilating nitrogen, in its reduced form, into the cell. Contigs encoding glutamine synthetase, specifically GSII, and glutamate synthase were present in *H. akashiwo* and some were significantly enriched under low N (ASC) (Table 3). The enrichment of GS-GOGAT cycle genes suggests the transcriptomic potential for ammonium assimilation. No contigs were identified as GSI or GSIII. The gene set (GSII and GLT) was enriched in the low N treatment, although this was not significantly different compared to the replete control (Kolmogorov-Smirnov test, $p = 0.08$) (Fig. 4D). In diatoms, GSI, II, and III have been identified, but the response of these genes to low N has been reported to be variable by species (Bender et al., 2014). Genes in the GS-GOGAT cycle have been found to be significantly upregulated under low N in several HAB species, including the dinoflagellates *Scrippsiella trochoidea* (GSII and GLT), *Karenia brevis* (GSIII), and *Alexandrium fundyense* (glutamine synthetase) (Morey et al., 2011; Zhuang et al., 2015; Cooper et al., 2016). Regulation of GS-GOGAT cycle genes is not always nutrient dependent. A ferredoxin-dependent glutamate synthase (GLT2) was detected (though not significantly enriched) in *A. anophagefferens* only when the cells were grown under low light, not under low N or low P conditions (Frischkorn et al., 2014).

In addition to surveying the transcriptomes for contigs involved in the transport and assimilation of inorganic nitrogen, contigs related to uptake of organic N in the form of urea were also identified to form another gene set. Urea transporters (DUR3), ureases, and multiple urease accessory proteins were identified and several urea transporters and a urease accessory protein (UreD) were significantly increased under low N (ASC) (Table 3). Overall, the gene set was significantly enriched under low N relative to the control (Kolmogorov-Smirnov test, $p = 0.0002$) (Fig. 4E). Enrichment of urea transporters, ureases and some accessory proteins in response to low N has been described in other marine phytoplankton, including *Aureococcus*, and some diatoms (Frischkorn et al., 2014; Zhuang et al., 2015; Cooper et al., 2016). Based on this work, *H. akashiwo* does not appear to express the full suite of urease accessory proteins, which includes UreD, UreG, and UreF, that in some eukaryotic species (e.g., *Arabidopsis sp.*) have been shown to be necessary for urease activation, and ultimately hydrolysis of urea to NO_3^- (Witte et al., 2005). This may explain why, although *H. akashiwo* can use urea as an N source (Herndon and Cochlan, 2007; Kudela et al., 2008), its preference for growth on urea is lower than that of NH_4^+ and NO_3^- (Herndon and Cochlan, 2007). Nevertheless, it is plausible that this species may shift to growth on urea when inorganic nitrogen is low. Urea delivery to coastal systems has and will continue to increase, given the global shift to the use of urea as the most common form of fertilizer and the increase in aquaculture facilities (Glibert et al., 2015 and references therein). Such a shift may influence growth dynamics and ichthyotoxicity in *H. akashiwo*, because cells cultured on urea were more ichthyotoxic than cells grown on NH_4^+ or low levels of NO_3^- (Matheson, 2014).

The urea cycle comprises a gene set that is distinct from the urea transporters described above. Except for arginase, contigs corresponding to a complete urea cycle were found in *H. akashiwo*, as previously described for diatoms (Armbrust et al., 2004), including a carbamoyl phosphate synthase (CPS3), ornithine carbamoyl transferase, argininosuccinate synthase, and argininosuccinate lyase (Table 3). Within these, only the ornithine carbamoyl transferase contigs were not significantly enriched under low N (ASC) (Table 3). Consequently, the gene set for the urea cycle was significantly enriched under low N, compared to the replete control (Kolmogorov-Smirnov, $p = 0.0002$) (Fig. 4F). Regulation of urea cycle genes is variable in other phytoplankton examined to date (Dyhrman et al., 2006; Allen et al., 2011; Bender et al., 2014). In diatoms, with the exception of the CPS gene, the majority of urea cycle genes were found to not respond to N limitation (Bender et al., 2014). In contrast, CPS in the prymnesiophyte *Prymnesium parvum* was differentially abundant under N stress, while other urea cycle genes, argininosuccinate synthase and argininosuccinate lyase, were identified as enriched under N stress (Liu et al., 2015a). Given this heterogeneity in expression patterns among phytoplankton, more work is warranted to resolve how the intracellular cycling of urea in *H. akashiwo* is modulated by the environment.

3.2.3. Differential abundance of P-specific genes

The raphidophyte *H. akashiwo* has a multifaceted response to low P, characterized by significantly enriched transcripts encoding genes involved in phosphate transport, phosphorus storage, organic P utilization, and the detoxification of arsenate. In all cases, individual contigs were tested for significant differential abundance using ASC, and then *a priori* defined 'gene sets' were examined using Kolmogorov-Smirnov tests to assess whether the pattern of contig abundance was significantly different from that of the replete control.

A common response to P stress in phytoplankton is to modulate the transport of phosphate via the induction of high affinity phosphate transporters, or via an increase in the number of P transporters (Lin et al., 2016 and references therein). Here, multiple *H. akashiwo* high affinity phosphate transporters (PHO4-like) (Table 4) were significantly more abundant (ASC) in the low P treatment relative to the control. The pattern of enriched contigs was confirmed for this gene set under low P (Kolmogorov-Smirnov test, $p = 0.008$) (Fig. 5A). This pattern is consistent with observations in other low P transcriptomes, including the *diatom*, *T. pseudonana*, and the HAB species, *A. anophagefferens* and *P. parvum* (Wurch et al., 2011a, 2011b; Dyhrman et al., 2012; Liu et al., 2015a).

Concomitant with the enrichment of a variety of inorganic phosphate transporters is the possibility that there could be an increase in cellular arsenate, as these transporters cannot typically discriminate between phosphate and arsenate (Budd and Craig, 1981; Silver and Phung, 2005). Contigs encoding components of an arsenite detoxification pathway, including arsenical resistance protein (arsH), arsenite translocating ATPase (arsA), and arsenate reductase (arsC) were detected in *H. akashiwo* and could mitigate arsenic toxicity during low P conditions (Table 4). The contigs annotated as arsC and arsH were significantly more abundant in the low P transcriptome, although the arsA contigs were not differentially abundant (Table 4). Although many contigs within this gene set were enriched in the low P treatment relative to the control, the trend was not significant (Kolmogorov-Smirnov test, $p = 0.14$) (Fig. 5B). These overall patterns of abundance are consistent with other phytoplankton (Dyhrman et al., 2012; Frischkorn et al., 2014) in low P cultures. Arsenic toxicity is tied to the As:P ratio (Saunders and Rocap, 2016), and would not typically be thought to occur in relatively high P coastal environments. However, the expression of a putative arsA has been detected in coastal populations of diatoms (Alexander et al.,

Table 4
Differential abundance of P-related contigs.

Functional Annotation	Contig IDs
Vacuolar transport chaperone (VTC4 homolog)	**2065, 4104, 36946, 39501**
PHO4-like (high affinity phosphate transporter)	**13010, 14470, 15213, 17963,** 23981, **34272,** 34390
Alkaline phosphatase	**33276**
PhoD-like alkaline phosphatase	12531, **13471**
Phosphatase	**39285**
5' Nucleotidase	36762, 39019
Arsenical resistance protein, arsH	**19475**
Arsenite translocating ATPase, arsA	1075, 19682
Arsenate reductase, arsC	**33062, 33893, 34231**

Contig IDs listed in bold were significantly enriched under low P. Contig IDs listed in bold were significantly enriched and those listed in italics were significantly less abundant under low P as determined by ASC (post-$p > 0.95$ and fold change > 2). Change in shading (light to dark grey) indicates gene sets presented in Fig. 5.

2015a), suggesting that this pathway warrants further scrutiny in field populations of *H. akashiwo*.

Genes putatively involved in changing cellular P allocation through polyphosphate production were found in *H. akashiwo* transcriptomes. Polyphosphates (polyP) are inorganic biopolymers of phosphate molecules linked by phosphoanhydride (P—O—P) bonds. The utility of polyphosphates to phytoplankton is thought to be quite diverse (e.g., metal chelation, mRNA processing and degradation, among other biological functions). In addition, their use as a reservoir for P is well established (Kornberg et al., 1999). Luxury uptake, or the storage of polyP for later use should P become depleted, occurs in the absence of any P stress (Karl and

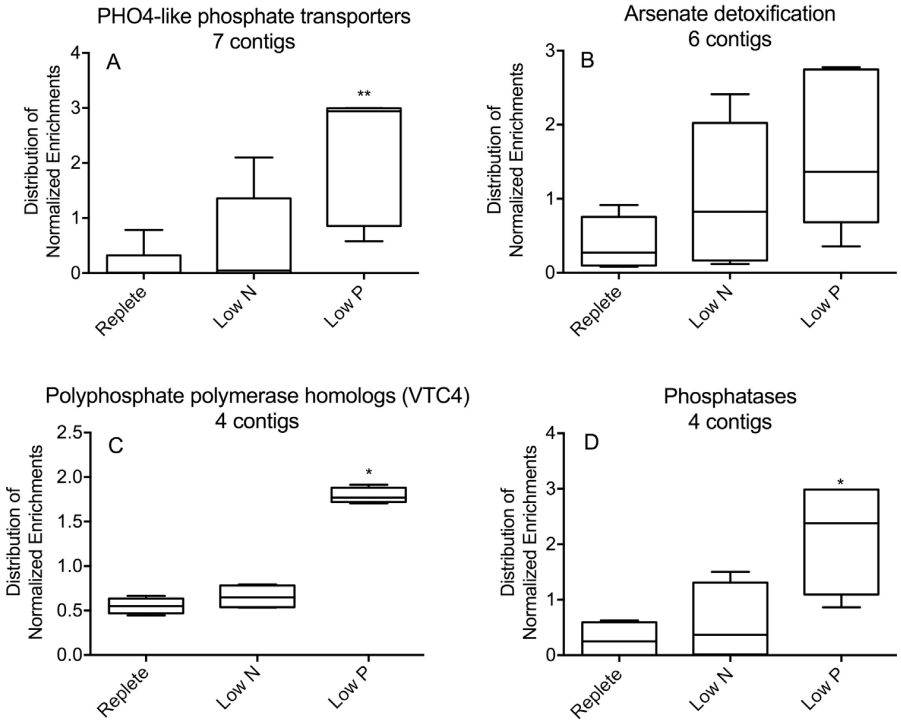

Fig. 5. Distribution of P-related gene sets, A) PHO4-like phosphate transporters, B) arsenate detoxification, C) polyphosphate polymerase homologs, and D) phosphatases. Distributions were compared using Kolmogorov-Smirnov tests. Whiskers show the normalized enrichment level for the least enriched, and most enriched contigs for each treatment within the gene set. Boxes encompass the normalized enrichment levels for the upper and lower 25th percentiles of contigs for each treatment within the module. The horizontal lines show the median normalized enrichment of contigs for each treatment within the module. Significance is indicated with asterisks, where one asterisk is $p < 0.05$, two asterisks are $p < 0.005$, three asterisks are $p < 0.0005$ and four asterisks are $p < 0.0001$.

Björkman, 2015). Eukaryotic polyP metabolism involves the vacuolar transporter chaperone (VTC) complex (Ogawa et al., 2000), where a recently identified polyphosphate polymerase within the complex generates polyphosphate by cleaving P from ATP (Hothorn et al., 2009). Four putative VTC4 homologs were identified in this study (Table 4). All were significantly more abundant at the contig level in the low P treatment (ASC) (Table 4) and also as a gene set (Kolmogorov-Smirnov test, $p = 0.03$) (Fig. 5C). A similar observation was reported for the marine diatom, *T. pseudonana* (Dyhrman et al., 2012). Microcosm and chemostat studies with *H. akashiwo* have demonstrated its ability to synthesize and store polyphosphate using ^{31}P NMR analysis (Miyata et al., 1986; Watanabe et al., 1988). Diel vertical migration for the purpose of P acquisition has been shown in *H. akashiwo*. Phosphate was stored as polyP from the P-rich bottom layer of the water column and later used for photophosphorylation during the daytime when *H. akashiwo* was in low P surface water (Watanabe et al., 1988). In this study, the gene expression patterns in the low P treatment were consistent with an increased allocation, not a decreased allocation of P to polyP. This counterintuitive result could be driven by intracellular cycling of polyP, where polyP is being utilized, but also synthesized to maintain intracellular standing stocks. In fact, polyP has been shown to be preferentially maintained over other P pools in the cell along a P gradient in the western North Atlantic (Martin et al., 2014).

A common strategy for growth in low P conditions observed in many phytoplankton (Dyhrman, 2016) is to switch from phosphate to growth on organic forms of P. This switch is typically mediated by phosphohydrolytic enzymes like phosphatases and 5′nucleotidases (Dyhrman and Palenik, 1999). For example, in this study alkaline phosphatase activity (APA) was significantly higher in low P cultures (0.0007 nmol P hr^{-1} cell^{-1}) compared to the replete control (0.0004 nmol P hr^{-1} cell^{-1}) (unpaired *t*-test, $p = 0.002$). A result that is similar to other independent observations (Wang and Liang, 2015). Consistent with the increase in APA, contigs for several putative phosphatases were significantly increased under low P (ASC) (Table 4). Overall, this gene set was also significantly enriched under low P compared to the replete control (Kolmogorov-Smirnov, $p = 0.03$) (Fig. 5D). Phosphomonoesters have been shown to support *H. akashiwo* growth as the sole P source (e.g., Yamaguchi et al., 2005; Wang et al., 2011), and this is likely mediated by the phosphatases observed herein. In contrast to other phytoplankton like *A. anophagefferens* and *T. pseudonana* (Dyhrman et al., 2012; Frischkorn et al., 2014), the *H. akashiwo* 5'nucleotidases did not show significant changes in relative abundance between low P and the replete control (Table 4).

4. Conclusion

The response of *H. akashiwo* to low N and low P elicited distinct changes in physiology and transcriptome patterns. Although often conceptualized in parallel, there was limited overlap in the transcriptional response to low N and P. The common stress responses largely included decreased relative abundance for transcripts related to photosynthesis and carbon fixation, consistent with reductions in growth rate. Under low N, many contigs and gene sets that were associated with N acquisition, transport and metabolism were enriched. In addition, the effect of N stress was also seen in other metabolic pathways, including those linked to changes in cellular phenotype, such as photosynthesis and glycosaminoglycan metabolism. In contrast, the pattern of response by *H. akashiwo* grown under low P was observed to be more targeted, with an increase in abundance of genes involved in P acquisition and transport. These results provide new insight into the genetic mechanisms that underpin nutrient stress responses in this HAB species and highlight the many differences between the responses to N and P stress. Diagnosing nutrient stress in phytoplankton populations during blooms has long been a goal of HAB research, and these results can be used to inform future field studies, linking transcriptional patterns to the physiological ecology of *H. akashiwo in situ*. Broadly, this work begins to address the long-term goal of developing a monitoring strategy for N and P stress that would aid in the management and prediction of *H. akashiwo* blooms.

Acknowledgements

The authors would like to thank Dr. Craig F. Aumack for processing the pCHO samples for this study. Support for this project has been provided in part by Woods Hole Oceanographic Institution Coastal Ocean Institute (COI) and World Surf League (WSL) PURE in partnership with Columbia University's Center for Climate and Life. Computational support was provided by the National Science Foundation under Grant Nos. DBI-1458641 and ABI-1062432 to Indiana University. The samples referenced in this study, MMETSP0292, MMETSP0294, and MMETSP0295 were sequenced, assembled and annotated with the ABySS pipeline at the National Center for Genome Resources with support from the Gordon and Betty Moore Foundation through Grant #2637 to the National Center for Genome Resources. This is LDEO contribution number 8137.[SS]

References

Alexander, H., Jenkins, B.D., Rynearson, T.A., Dyhrman, S.T., 2015a. Metatranscriptome analyses indicate resource partitioning between diatoms in the field. Proc. Natl. Acad. Sci. U. S. A. 112, E2182–E2190.
Alexander, H., Rouco, M., Haley, S.T., Wilson, S.T., Karl, D.M., Dyhrman, S.T., 2015b. Functional group-specific traits drive phytoplankton dynamics in the oligotrophic ocean. Proc. Natl. Acad. Sci. U. S. A. 112, E5972–E5979.
Allen, A.E., Dupong, C.L., Obornik, M., Horák, A., Nunes-Nesi, A., McCrow, J.P., Zheng, H., Johnson, D.A., Hu, H., Fernie, A.R., Bowler, C., 2011. Evolution and metabolic significance of the urea cycle in photosynthetic diatoms. Nature 473, 203–209.
Altschul, S.F., Gish, W., Miller, W., Myers, E.W., Lipman, D.J., 1990. Basic local alignment search tool. J. Mol. Biol. 215, 403–410.
Anders, S., Pyl, T.P., Huber, W., 2014. HTSeq – a python framework to work with high-throughput sequencing data. Bioinformatics 31, 166–169.
Anderson, D.M., Burkholder, J.M., Cochlan, W.P., Glibert, P.M., Gobler, C.J., Heil, C.A., Kudela, R.M., Parsons, M.L., Rensel, J.E.J., Townsend, D.W., Trainer, V.L., Vargo, G. A., 2008. Harmful algal blooms and eutrophication: examining linkages from selected coastal regions of the United States. Harmful Algae 8, 39–53.
Anderson, D.M., Keafer, B.A., Kleindinst, J.L., McGillicuddy Jr., D.J., Martin, J.L., Norton, K., Pilskaln, C.H., Smith, J.A., Sherwood, C.R., Butman, B., 2014. *Alexandrium fundyense* cysts in the Gulf of Maine: Long-term time series of abundance and distribution, and linkages to past and future blooms. .
Armbrust, E.V., Berges, J.A., Bowler, C., Green, B.R., Martinez, D., Putnam, N.H., Zhou, S., Allen, A.E., Apt, K.E., Bechner, M., Brzezinski, M.A., Chaal, B.K., Chiovitti, A., Davis, A.K., Demarest, M.S., Detter, J.C., Glavina, T., Goodstein, D., Hadi, M.Z., Hellsten, U., Hildebrand, M., Jenkins, B.D., Jurka, J., Kapitonov, V.V., Kroger, N., Lau, W.W.Y., Lane, T.W., Larimer, F.W., Lippmeier, J.C., Lucas, S., Medina, M., Montsant, A., Obornik, M., Parker, M.S., Palenik, B., Pazour, G.J., Richardson, P.M., Rynearson, T.A., Saito, M.A., Schwartz, D.C., Thamatrakoln, K., Valentin, K., Vardi, A., Wilkerson, F.P., Rokhsar, D.S., 2004. The genome of the diatom *Thalassiosira pseudonana*: Ecology, evolution and metabolism. Science 306, 79–86.
Bateman, A., 2004. The Pfam protein families database. Nucleic Acids Res. 32, 138D–141D.
Bender, S.J., Durkin, C.A., Berthiaume, C.T., Morales, R.L., Armbrust, E.V., 2014. Transcriptional responses of three model diatoms to nitrate limitation of growth. Front. Mar. Sci. 1, 1–15.
Berg, G.M., Shrager, J., Glockner, G., Arrigo, K.R., Grossman, A.R., 2008. Understanding nitrogen limitation in *Aureococcus anophagefferens* (Pelagophyceae) through cDNA and qRT-PCR analysis. J. Phycol. 5, 1235–1249.
Berges, J.A., 1997. Minireview: algal nitrate reductases. Eur. J. Phycol. 32, 3–8.
Biswas, S., Agrawal, Y.N., Mucyn, T.S., Dangl, J.L., Jones, C.D., 2013. Biological averaging in RNA-seq. Quant. Methods arXiv:1309.0670 [q-bio.QM].
Budd, K., Craig, S.R., 1981. Resistance to arsenate toxicity in the blue-green alga *Synechococcus leopoliensis*. Botany 59, 1518–1521.
Cai, H., Lu, Y., Xie, W., Zhu, T., Lian, X., 2012a. Transcriptome response to nitrogen starvation in rice. J. Biosci. 37, 731–747.
Cai, H., Xie, W., Zhu, T., Lian, X., 2012b. Transcriptome response to phosphorus starvation in rice. Acta Physiol. Plant. 334, 327–341.

Chang, F.H., Anderson, C., Boustead, N.C., 1990. 1st record of a *Heterosigma* (Raphidophyceae) bloom with associated mortality of cage-reared salmon in Big Glory Bay, New Zealand. New Zeal. J. Mar. Freshwater Res. 24, 461–469.

Cooper, J.T., Sinclair, G.A., Wawrik, B., 2016. Transcriptome analysis of *Scrippsiella trochoidea* CCMP 3099 reveals physiological changes related to nitrate depletion. Front. Microbiol. 7, 1–19.

Coyne, K.J., 2010. Nitrate reductase (NR1) sequence and expression in the harmful alga *Heterosigma akashiwo* (Raphidophyceae). J. Phycol. 46, 135–142.

De Jesus Raposo, M.F., de Morais, R.M.S.C., de Morais, A.M.M.B., 2013. Bioactivity and applications of sulphated polysaccharides from marine microalgae. Mar. Drugs. 11, 233–252.

Dubois, M., Gilles, K.A., Hamilton, J.K., Rebers, P.A., Smith, F., 1956. Colorimetric method for determination of sugars and related substances. Anal. Chem. 28, 350–356.

Dyhrman, S.T., Palenik, B., 1999. Phosphate stress in cultures and field populations of the dinoflagellate *Prorocentrum minimum* detected by a single-cell alkaline phosphatase assay. Appl. Environ. Microbiol. 65, 3205–3212.

Dyhrman, S.T., Ruttenberg, K.C., 2006. Presence and regulation of alkaline phosphatase activity in eukaryotic phytoplankton from the coastal ocean: implications for dissolved organic phosphorus remineralization. Limnol. Oceanogr. 51, 1381–1390.

Dyhrman, S.T., Haley, S.T., Birkeland, S.R., Wurch, L.L., Cipriano, M.J., McArthur, A.G., 2006. Long serial analysis of gene expression for gene discovery and transcriptome profiling in the widespread marine coccolithophore *Emiliania huxleyi*. Appl. Environ. Microbiol. 72, 252–260.

Dyhrman, S.T., Jenkins, B.D., Rynearson, T.A., Saito, M.A., Mercier, M.L., Alexander, H., Whitney, L.P., Drzewianowski, A., Bulygin, V., Bertrand, E.M., Wu, Z., Benitez-Nelson, C., Heithoff, A., 2012. The transcriptome and proteome of the diatom *Thalassiosira pseudonana* reveal a diverse phosphorus stress response. PLoS One 7, e33768.

Dyhrman, S.T., 2016. The Physiology of Microalgae. In: Borowitzka, M.A., Beardall, J., Raven, J.A. (Eds.), Springer, New York, USA, pp. 155–183.

Engel, A., Piontek, J., Grossart, H.-P., Riebesell, U., Schulz, K.G., Sperling, M., 2014. Impact of CO_2 enrichment on organic matter dynamics during nutrient induced coastal phytoplankton blooms. J. Plankt. Res. 36, 641–657.

Engel, A., 2000. The role of transparent exopolymer particles (TEP) in the increase in apparent particle stickiness (α) during the decline of a diatom bloom. J. Plankt. Res. 22, 485–497.

Frischkorn, K.R., Harke, M.J., Gobler, C.J., Dyhrman, S.T., 2014. De novo assembly of *Aureococcus anophagefferens* transcriptomes reveals diverse responses to the low nutrient and low light conditions present during blooms. Front. Microbiol. 5, 1–16.

Gandhi, N.S., Mancera, R.L., 2008. The structure of glycosaminoglycans and their interactions with proteins. Chem. Biol. Drug Des. 72, 455–482.

Glibert, P.M., Flemer, D., Paerl, H., 2010. Nutrients in Estuaries: A Summary Report of the National Estuarine Experts Workgroup 2005–2007. In: Glibert, P.M., Madden, C.J., Boynton, W., Flemer, D., Heil, C., Sharp, J. (Eds.), Environmental Protection Agency, Washington, D.C, pp. 11–26.

Glibert, P.M., Wilkerson, F.P., Dugdale, R.C., Raven, J.A., Dupont, C.L., Leavitt, P.R., Parker, A.E., Burkholder, J.M., Kana, T.M., 2015. Pluses and minuses of ammonium and nitrate uptake and assimilation by phytoplankton and implications for productivity and community composition, with emphasis on nitrogen-enriched conditions. Limnol. Oceanogr. 1, 165–197.

Gobler, C.J., Berry, D.L., Dyhrman, S.T., Wilhelm, S.W., Salamov, A., Lobanov, A.V., Zhang, Y., Collier, J.L., Wurch, L.L., Kustka, A.B., Dill, B.D., Shah, M., VerBermoes, N.C., Kuo, A., Terry, A., Pangilinan, J., Lindquist, E.A., Lucas, S., Paulsen, I.T., Hattenrath-Lehmann, T.K., Talmage, S.C., Walker, E.A., Koch, F., Burson, A.M., Marcoval, M.A., Tang, Y.Z., LeClair, G.R., Coyne, K.J., Berg, G.M., Bertrand, E.M., Saito, M.A., Gladyshev, V.N., Grigoriev, I.V., 2011. Niche of harmful alga *Aureococcus anophagefferens* revealed through ecogenomics. Proc. Natl. Acad. Sci. U. S. A. 108, 4352–4357.

Gough, J., Karplus, K., Hughey, R., Chothia, C., 2001. Assignment of homology to genome sequences using a library of hidden Markov models that represent all proteins of known structure. J. Mol. Biol. 313, 903–919. doi:http://dx.doi.org/10.1006/jmbi.2001.5080.

Haft, D.H., Loftus, B.J., Richardson, D.L., Yang, F., Eisen, J.A., Paulsen, I.T., et al., 2001. TIGRFAMs: a protein family resource for the functional identification of proteins. Nucleic Acids Res. 29, 41–43.

Harke, M.J., Gobler, C.J., 2013. Global transcriptional responses of the toxic cyanobacterium, *Microcystis aeruginosa*, to nitrogen stress, phosphorus stress, and growth on organic matter. PLoS One 8, e69834.

Herndon, J., Cochlan, W.P., 2007. Nitrogen utilization by the raphidophyte *Heterosigma akashiwo*: growth and uptake kinetics in laboratory cultures. Harmful Algae 6, 260–270.

Honjo, T., 1992. Harmful red tides of *Heterosigma akashiwo*. In: Svrjecek, R.S. (Ed.), Control of Disease in Aquaculture. NOAA Technical Report NMFS 111, 27-32.

Honjo, T., 1993. Overview on bloom dynamics and physiological ecology of *Heterosigma akashiwo*. In: Smayda, T.J., Shimizu, Y. (Eds.), Toxic Phytoplankton Blooms in the Sea. Elsevier, New York, NY, USA, pp. 33–41.

Hothorn, M., Neumann, H., Lenherr, E.D., Wehner, M., Rybin, V., Hassa, P.O., Uttenweiler, A., Reinhardt, M., Schmidt, A., Seiler, J., Ladurner, A.G., Herrmann, C., Scheffzek, K., Mayer, A., 2009. Catalytic core of a membrane-associated eukaryotic polyphosphate polymerase. Science 324, 513–516.

Huang, L.K., Yan, H.D., Zhao, X.X., Zhang, X.Q., Wang, J., Frazier, T., Yin, G., Huang, X., Yan, D.F., Zang, W.J., Ma, X., Peng, Y., Yan, Y.H., Liu, W., 2015. Identifying differentially expressed genes under heat stress and developing molecular markers in orchardgrass (*Dactylis glomerata* L.) through transcriptome analysis. Mol. Ecol. Resour. 15, 1497–1509.

Huang, X., 1999. CAP3: a DNA sequence assembly program. Genome Res. 9, 868–877.

Jeong, H.J., Seong, K.A., Kang, N.S., Yoo, Y.D., Nam, S.W., Park, J.Y., Shin, W., Glibert, P. M., John, D., 2010. Feeding by raphidophytes on the cyanobacterium *Synechococcus* sp. Aquat. Microb. Ecol. 58, 181–195.

Jeong, H.J., Lim, A.S., Franks, P.J.S., Lee, K.H., Kim, J.H., Kang, N.S., Lee, M.J., Jang, S.H., Lee, S.Y., Yoon, E.Y., Park, J.Y., Yoo, Y.D., Seong, K.D., Kwon, J.E., Jang, T.Y., 2015. A hierarchy of conceptual models of red-tide generation Nutrition, behavior, and biological interactions. Harmful Algae 47, 97–115.

Jeong, H.J., 2011. Mixotrophy in red tide algae raphidophytes. J. Eukaryot. Microbiol. 58, 215–222.

Johnson, J.G., Morey, J.S., Neely, M.G., Ryan, J.C., Van Dolah, F.M., 2012. Transcriptome remodeling associated with chronological aging in the dinoflagellate *Karenia brevis*. Mar. Genomics 5, 15–25.

Kamiyama, T., Itakura, S., Nagasaki, K., 2000. Changes in microbial loop components: effects of a harmful algal bloom formation and its decay. Aquat. Microb. Ecol. 21, 21–30.

Kamiyama, T., 1995. Change in the microzooplankton community during decay of a *Heterosigma akashiwo* bloom. J. Oceanogr. 51, 279–287.

Kanehisa, M., 2006. From genomics to chemical genomics: new developments in KEGG. Nucleic Acids Res. 34, D354–D357.

Karl, D.M., Björkman, K.M., 2015. Dynamics of dissolved organic phosphorus, In: Hansell, D.A., Carlson, C.A. (Eds.), Biogeochemistry of Marine Dissolved Organic Matter. 2nd edition Academic Press Ltd – Elsevier Science Ltd, London, pp. 233–334.

Keeling, P.J., Burki, F., Wilcox, H.M., Allam, V., Allen, E.E., Amaral-Zettler, L.A., et al., 2014. The marine microbial eukaryote transcriptome sequencing project (MMETSP): illuminating the functional diversity of eukaryotic life in the oceans through transcriptome sequencing. PLoS Biol. 12, e1001889.

Kempton, J., Keppler, C.J., Lewitus, A., Shuler, A., Wilde, S., 2008. A novel *Heterosigma akashiwo* (Raphidophyceae) bloom extending from a South Carolina bay to offshore waters. Harmful Algae 7, 235–240.

Keppler, C.J., Hoguet, J., Smith, K., Ringwood, A.H., Lewitus, A.J., 2005. Sublethal effects of the toxic alga *Heterosigma* akashiwo on the southern oyster (*Crassostrea virginica*). Harmful Algae 4, 275–285.

Koid, A.E., Liu, Z., Terrado, R., Jones, A.C., Caron, D.C., Heidelberg, K.B., 2014. Comparative transcriptome analysis of four prymnesiophyte algae. PLoS One 9, e97801.

Konotchick, T., Dupont, C.L., Valas, R.E., Badger, J.H., Allen, A.E., 2013. Transcriptomic analysis of metabolic function in the giant kelp, *Macrocystis pyrifera*, across depth and season. New Phytol. 198, 398–407.

Kopf, M., Möke, F., Bauwe, H., Hess, W.R., Hagemann, M., 2015. Expression profiling of the bloom-forming cyanobacterium *Nodularia* CCY9414 under light and oxidative stress conditions. ISME J. 9, 2139–2152.

Kornberg, A.A., Rao, N.N., Ault-Riché, D., 1999. Inorganic polyphosphate: a molecule of many functions. Annu. Rev. Biochem. 68, 89–125.

Kudela, R.M., Lane, J.Q., Cochlan, W.P., 2008. The potential role of anthropogenically derived nitrogen in the growth of harmful algae in California, USA. Harmful Algae 8, 103–110.

Langmead, B., Salzberg, S.L., 2012. Fast gapped-read alignment with bowtie 2. Nature 9, 357–359.

Li, W., Godzik, A., 2006. Cd-hit: a fast program for clustering and comparing large sets of protein or nucleotide sequences. Bioinformatics 22, 1658–1659.

Li, L., Stoockert, C., Roos, D., 2003. OrthoMCL: identification of ortholog groups for eukaryotic genomes. Genome Res. 13, 2178–2189.

Li, R., Li, Y., Kristiansen, K., Wang, J., 2008. SOAP: Short oligonucleotide alignment program. Bioinformatics 24, 713–714.

Lin, S., Litaker, R.W., Sunda, W.G., 2016. Phosphorus physiological ecology and molecular mechanisms in marine phytoplankton. J. Phycol. 52, 10–36.

Lindner, R., Friedel, C.C., 2012. A comprehensive evaluation of alignment algorithms in the context of RNA-seq. PLoS One 7, e52403.

Liu, Z., Koid, A.E., Terrado, R., Campbell, V., Caron, D.A., Heidelberg, K.B., 2015a. Changes in gene expression of *Prymnesium parvum* induced by nitrogen and phosphorus limitation. Front. Microbiol. 6, 1–15.

Liu, Y., Chen, T., Song, S., Li, C., 2015b. Effects of nitrogenous nutrition on growth and assimilation enzymes of dinoflagellate *Akashiwo sanguinea*. Harmful Algae 50, 99–106.

Lopes, D.C., Maurer, J.B.B., Stevan-Hancke, F.R., de Oliveira Proença, L.A., Zawadzki-Baggio, S.F., 2012. Chemical analysis of exopolysaccharide fractions and lipid compounds of the microalga *Heterosigma akashiwo* grown in vitro. Bot. Mar. 55, 565–580.

MacIntyre, H.L., Cullen, J.J., 2005. Using cultures to investigate the physiological ecology of microalgae. In: Andersen, R.A. (Ed.), Algal Culturing Techniques. Elsevier Academic Press Burlington, MA, USA, pp. 287–326.

Martin, P., Dyhrman, S.T., Lomas, M.W., Poulton, N.J., Van Mooy, B.A.S., 2014. Accumulation and enhanced cycling of polyphosphate by Sargasso Sea plankton in response to low phosphorus. Proc. Natl. Acad. Sci. USA 22, 8089–8094.

Matheson, J.R., 2014. The Effects of Ocean Acidification and Eutrophication on the Growth, Lipid Composition and Toxicity of the Marine Raphidophyte *Heterosigma akashiwo*. Ph.D. Thesis. University of Western Ontario, Ontario, Canada.

Miyata, K., Hattori, A., Ohtsuki, A., 1986. Variation of cellular phosphorus composition of *Skeletonema costatum* and *Heterosigma akashiwo* grown in chemostats. Mar. Biol. 93, 291–297.

Mohamed, Z.A., Al-Shehri, A.M., 2012. The link between shrimp farm runoff and blooms of toxic *Heterosigma akashiwo* in Red Sea coastal waters. Oceanologia 54, 287–309.

Morey, J.S., Monroe, E.A., Kinney, A.L., Beal, M., Johnson, J.G., Hitchcock, G.L., Van Dolah, F.M., 2011. Transcriptomic response of the red tide dinoflagellate, *Karenia brevis*, to nitrogen and phosphorus depletion and addition. BMC Genomics 1, 346–363.

Nygaard, K., Tobeisen, A., 1993. Bacterivory in algae – a survival strategy during nutrient limitation. Limnol. Oceanogr. 38, 273–279.

Ogawa, N., DeRisi, J., Brown, P.O., 2000. New components of a system for phosphate accumulation and polyphosphate metabolism in *Saccharomyces cerevisiae* revealed by genomic expression analysis. Mol. Biol. Cell. 11, 4309–4321.

Parkhill, J.P., Maillet, G., Cullen, J.J., 2001. Fluorescence-based maximal quantum yield for PSII as a diagnostic of nutrient stress. J. Phycol. 37, 517–529.

Rensel, J.E.J., Haigh, N., Tynan, T.J., 2010. Fraser river sockeye salmon marine survival decline and harmful blooms of *Heterosigma akashiwo*. Harmful Algae 10, 98–115.

Saunders, J.K., Rocap, G., 2016. Genomic potential for arsenic efflux and methylation varies among global *Prochlorococcus* populations. ISME J. 10, 197–209.

Senni, K., Pereira, J., Gueniche, F., Delbarre-Ladrat, C., Sinquin, C., Ratiskol, J., Godeau, G., Fischer, A.-M., Helly, D., Colliec-Jouault, S., 2011. Marine polysaccharides: a source of bioactive molecules for cell therapy and tissue engineering. Mar. Drugs 9, 1664–1681.

Silver, S., Phung, L.T., 2005. Minireview: genes and enzymes involved in bacterial oxidation and reduction of inorganic arsenic. Appl. Environ. Microbiol. 71, 599–608.

Simpson, J.T., Durbin, R., 2012. Efficient *de novo* assembly of large genomes using compressed data structures. Genome Res. 22, 549–556.

Simpson, J.T., Wong, K., Jackman, S.D., Schein, J.E., Jones, S.J.M., Birol, I., 2009. ABySS: a parallel assembler for short read sequence data. Genome Res. 19, 1117–1123.

Smayda, T., 1990. Novel and nuisance phytoplankton blooms in the sea – evidence for a global epidemic. In: Graneli, E., Sundstrom, B., Edler, L., Anderson, D.M. (Eds.), Toxic Marine Phytoplankton. Elsevier, New York, pp. 29–40.

Smayda, T., 1998. Ecophysiology and bloom dynamics of *Heterosigma akashiwo* (Raphidophyceae). In: Anderson, D.M., Cembella, A.D., Hallegraeff, G.M. (Eds.), Physiological Ecology of Harmful Algal Blooms. Springer, New York, pp. 113–131.

Smith, G.J., Zimmerman, R.C., Alberte, R.S., 1992. Molecular and physiological responses of diatoms to variable levels of irradiance and nitrogen availability: growth of *Skeletonema costatum* in simulated upwelling conditions. Limnol. Oceanogr. 37, 989–1007.

Spungin, D., Pfreundt, U., Berthelot, H., Bonnet, S., AlRoumi, D., Natale, F., Hess, W.R., Bidle, K.D., Berman-Frank, I., 2016. Mechanisms of *Trichodesmium* demise within the New Caledonian lagoon during the VAHINE mesocosm experiment. Biogeosciences 13, 4187–4203.

Stewart, J.J., Coyne, K.J., 2011. Analysis of raphidophyte assimilatory nitrate reductase reveals unique domain architecture incorporating a 2/2 hemoglobin. Plant Mol. Biol. 77, 565–575.

Stewart, J.J., 2011. Nitrate Reductase Sequence Analysis and Expression in the Raphidophytes, Heterosigma Akashiwo and *Chattonella Subsalsa*. Ph.D. Thesis. University of Delaware, Delaware, USA.

Strickland, J.D.H., Parsons, T.R., 1972. A Practical Handbook of Seawater Analyses, 2nd ed. Fisheries Research Board of Canada, Ottawa.

Subramanian, A., Tamayo, P., Mootha, V.K., Mukherjee, S., Ebert, B.L., Gillette, M.A., Paulovich, A., Pomeroy, S.L., Golub, T.R., Lander, E.S., Mesirov, J.P., 2005. Gene set enrichment analysis: a knowledge-based approach for interpreting genome-wide expression profiles. Proc. Natl. Acad. Sci. 102, 15545–15550.

Taylor, F.J.R., Haigh, R., 1993. The ecology of fish-killing blooms of the chloromonad flagellate *Heterosigma* in the strait of Georgia and adjacent waters. In: Smayda, T.J., Shimizu, Y. (Eds.), Toxic Phytoplankton Blooms in the Sea. Toxic Phytoplankton Blooms in the Sea. Elsevier, New York, NY, USA, pp. 705–710.

Thomas, M.F., Abdul-Wajid, S., Panduro, M., Babiarz, J.E., Rajaram, M., Woodruff, P., et al., 2012. Eri1 regulates microRNA homeostasis and mouse lymphocyte development and antiviral function. Blood 120, 130–142.

Verity, P.G., Stoecker, D., 1982. Effects of *Olisthodiscus luteus* on the growth and abundance of tintinnids. Mar. Biol. 72, 79–87.

Voss, M., Baker, A., Bange, H.W., Conley, D., Cornell, S., Deutsch, B., Engel, A., Ganeshram, R., Garnier, J., Heiskanen, A.-S., Jickells, T., Lancelot, C., McQuatters-Gollop, A., Middelburg, J., Schiedek, D., Slomp, C.P., Conley, D.P., 2011. The European Nitrogen Assessment. In: Sutton, M.A., Howard, C.M., Erisman, J.W., Billen, G., Bleeker, A., Greenfelt, P., Van Grinsven, H., Grizzeti, B. (Eds.), Cambridge University Press, Cambridge, UK, pp. 147–176.

Wang, Z., Liang, Y., 2015. Growth and alkaline phosphatase activity of *Chattonella marina* and *Heterosigma akashiwo* in response to phosphorus limitation. J. Environ. Sci. 28, 1–7.

Wang, Z., Liang, Y., Kang, W., 2011. Utilization of dissolved organic phosphorus by different groups of phytoplankton taxa. Harmful Algae 12, 113–118.

Watanabe, M., Kohata, K., Kunugi, M., 1988. Phosphate accumulation and metabolism by *Heterosigma akashiwo* (Raphidophyceae) during diel vertical migration in a stratified microcosm. J. Phycol. 24, 22–28.

Witte, C.-P., Rosso, M.G., Romeis, T., 2005. Identifcation of three urease accessory proteins that are required for urease activation in *Arabidopsis*. Plant Physiol. 139, 1155–1162.

Wu, Z., Jenkins, B.D., Rynearson, T.A., Dyhrman, S.T., Saito, M.A., Mercier, M., Whitney, L.P., 2010. Empirical bayes analysis of sequencing-based transcriptional profiling without replicates. BMC Bioinf. 11, 564.

Wurch, L.L., Haley, S.T., Orchard, E.D., Gobler, C.J., Dyhrman, S.T., 2011a. Nutrient-regulated transcriptional responses in the brown tide-forming alga *Aureococcus anophagefferens*. Environ. Microbiol. 13, 468–481.

Wurch, L.L., Bertrand, E.M., Saito, M.A., Van Mooy, B.A.S., Dyhrman, S.T., 2011b. Proteome changes driven by phosphorus deficiency and recovery in the brown tide-forming alga *Aureococcus anophagefferens*. PLoS One 6, e28949.

Yamaguchi, H., Sakou, H., Fukami, K., Adachi, M., Yamaguchi, M., Nishijima, T., 2005. Utilization of organic phosphorus and production of alkaline phosphatase by the marine phytoplankton, *Heterocapsa circularisquama*, *Fibrocapsa japonica* and *Chaetoceros ceratosporum*. Plankton Biol. Ecol. 52, 67–75.

Zhang, Z., Wood, W.I., 2003. A profile hidden Markov model for signal peptides generated by HMMER. Bioinformatics 19, 307–308.

Zhang, Y., Fu, F.-X., Whereat, E., Coyne, K.J., Hutchins, D.A., 2006. Bottom-up controls on a mixed-species HAB assemblage: a comparison of sympatric *Chattonella subsalsa* and *Heterosigma akashiwo* (Raphidophyceae) isolates from the Delaware Inland Bays, USA. Harmful Algae 5, 310–320.